

# Nanolithography Using Protease Etching of Protein Surfaces

Rodica E. Ionescu, Robert S. Marks, and Levi A. Gheber\*

*The Institute for Applied Biosciences and Department of Biotechnology Engineering, Ben-Gurion University of the Negev, P.O. Box 653, Beer-Sheva 84105, Israel*

*Received August 10, 2003; Revised Manuscript Received October 7, 2003*

## ABSTRACT

We present for the first time the use of a proteolytic enzyme to create nanometer-size depressions in a protein surface. This was achieved by delivering trypsin via a nanopipet, controlled with a scanning probe microscope, to a dried bovine serum albumin film. We suggest a comprehensive model, explaining the processes involved and providing ways to control the parameters governing them. Enzyme nanolithography should be useful in areas of nanobiotechnology, such as nanobiochips, nanofluidics, and lab-on-a-chip.

Harnessing biological molecular machinery to produce nanoscale features and devices is an exciting avenue, an alternative approach to designing nanomachines *de novo*, and a scope of nanobiotechnology. Making use of high recognition specificity by various classes of biological molecules, “smart” building blocks, one can create nanoscale structures of high complexity. For example, very interesting applications have been proposed and demonstrated with DNA, showing very specific addressing and self-assembling properties.<sup>1,2</sup> On another approach, scanning probe microscopy (SPM) techniques have been shown to be very useful in creating nanoscale patterns of biomolecules, due to their high spatial precision. The nano fountain pen (NFP)<sup>3</sup>, able to deliver minute amounts of liquids to various surfaces, has been used to print nanoscale features of photoresist,<sup>4</sup> DNA,<sup>5</sup> or proteins.<sup>6</sup> Dip pen nanolithography (DPN),<sup>7</sup> where an atomic force microscope (AFM) probe is dipped in a solution of self-assembling molecules and then used to write nanometric patterns, has been used to print proteins,<sup>8,9</sup> polymers,<sup>10</sup> or DNA.<sup>11</sup> Also, light-based techniques,<sup>12,13</sup> using near-field scanning optical microscopy (NSOM) may be very useful to patterning with biological molecules. Here we combine biological specificity with precise positioning offered by NFP, to realize enzyme-based negative lithography (creation of depressions) at nanometer scales.

Enzymes are a large class of biological molecules that have not yet been addressed in the context of nanofabrication, although they present, in our view, a much richer spectrum of specific interactions than does, e.g., DNA. Enzymes are “nanochemists”, able to promote chemical reactions with high specificity, efficiency and yield. Particularly, proteolytic enzymes hydrolyze peptide bonds, thereby cleaving proteins at very specific sites along the amino acid sequence. We used trypsin, a proteolytic enzyme that cleaves on the

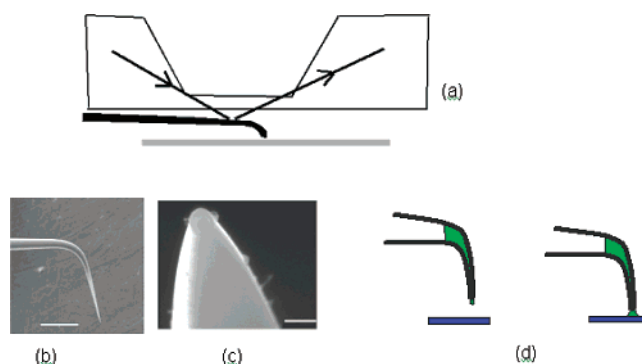


**Figure 1.** Nanofountain pen (NFP) setup. (a) SPM scanning head, holding the nanopipet as its probe and controlling it using standard AFM methods. (b) SEM image of a cantilevered nanopipet. Scale bar: 100  $\mu\text{m}$ . (c) Close-up of the tapered end of a 50 nm aperture nanopipet. Scale bar: 500 nm. (d) When the pipet is filled with liquid, it runs to the tapered tip due to capillary forces, but does not flow out due to surface tension (left panel). However, upon contacting the surface, the liquid flows out to the substrate (right panel).

carboxyl side of lysine and arginine residues, to break locally a layer of bovine serum albumin (BSA). BSA is a 607 amino acid protein, which contains 60 lysines and 26 arginines with the longest peptide between two adjacent cleavage sites of 20 amino acids in length (amino acid sequence available as Supporting Information); thus, a major collapse of the three-dimensional structure of BSA is expected after cleavage. We prepared substrates by dissolving 0.5 mM BSA (Sigma) in ultrapure Millipore water and applying 35  $\mu\text{L}$  drops onto 95% ethanol flamed glass cover slips, then allowed to dry for 7 days at room temperature. Bovine trypsin, treated with L-(tosylamido-2-phenyl ethyl) chloromethyl ketone, to inhibit chemotryptic activity (TPCK-trypsin, bovine pancreas, Pierce), in an amount of 1.3 mg, was diluted in 1 mL of 0.05 M sodium borate, pH = 8.5 (BupH Borate buffer, Pierce) and

\* Corresponding author. E-mail: glevi@bgumail.bgu.ac.il

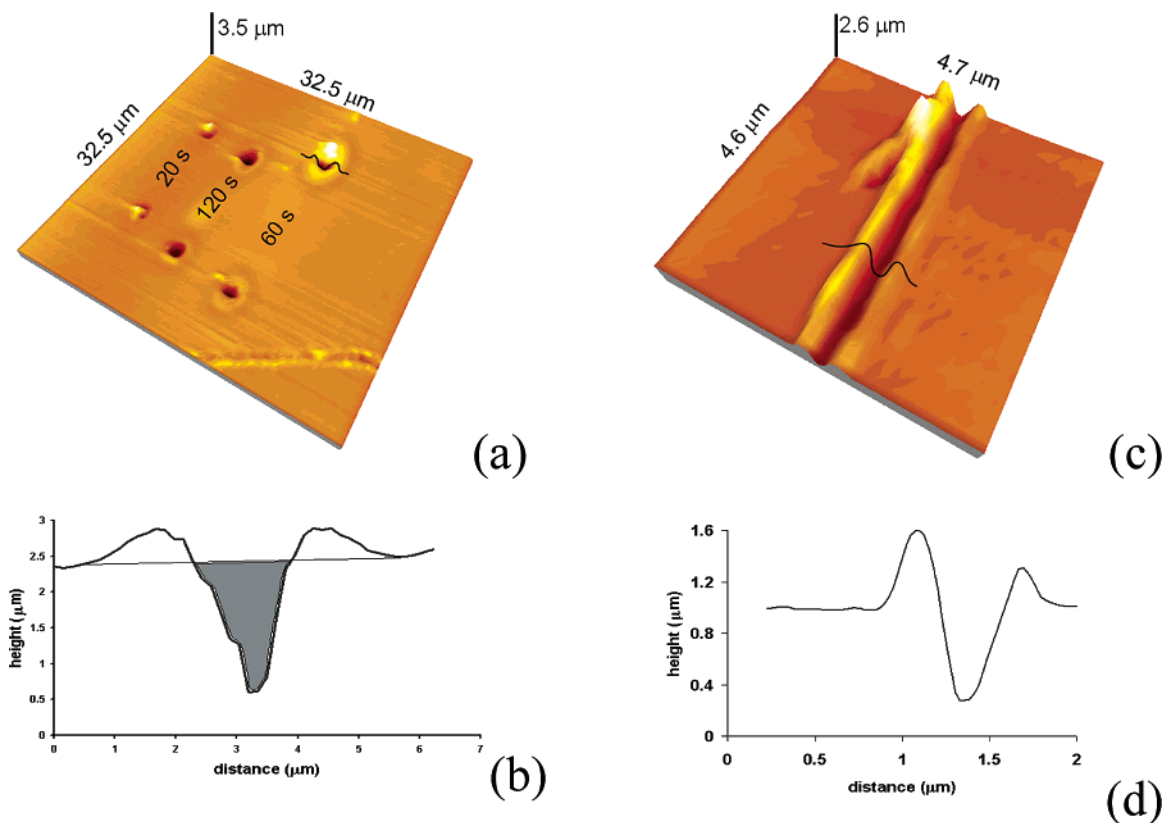


**Figure 2.** AFM images of features created by flowing trypsin to the BSA substrate. (a) Wells of various dimensions, created by flowing trypsin solution through a 200 nm pipet for different time durations (20, 60, and 120 s, as indicated in the figure), have widths of 0.6, 1.2, and 2.3  $\mu\text{m}$  and depths of 0.9, 1.9, and 2.4  $\mu\text{m}$ , respectively. (b) Cross-section of a 60 s well in (a), along the line indicated. Shaded area indicates the volume of the well that was considered for calculation. (c) Channel created by flowing trypsin solution through a 50 nm pipet. (d) Cross-section of the channel in (c), along the line indicated, shows a width of  $\sim 340$  nm and a depth of  $\sim 660$  nm.

subsequently loaded in the nanopipets (Nanonics Ltd., Jerusalem, Israel). Trypsin was flown through a cantilevered nanopipet to the BSA film surface and allowed to engrave features. The process was controlled with nanometer precision by employing a SPM flat scanner, (Figure 1a) (“NSOM/AFM 100” – Nanonics Ltd., Jerusalem, Israel), to hold the nanopipet (Figure 1b, c) and position the sample in a “nano fountain pen” (NFP) fashion<sup>3–6</sup> (Figure 1d) (real time writing movie available as Supporting Information). Subsequently, the same instrument was used to image the features with standard atomic force microscope (AFM) probes (MikroMasch, Tallinn, Estonia).

Round wells, with increasing diameters and depths, resulted from keeping the nanopipet in contact with the BSA substrate for increasing periods of time. In Figure 2a we present an AFM image showing three pairs of wells created this way. A cross-section through one of the wells is shown in Figure 2b. The volumes of the depressions below the surface of the sample (as shown in the shaded area in Figure 2b) were calculated and appear to depend roughly linearly with the time of trypsin flow, as shown in Figure 4b. The negative values of the volumes indicate a depression. These experiments were repeated with nanopipets having different aperture diameters, with similar results.

Channels were created by moving the sample while the pipet was in contact. Their dimensions were found to depend on the diameter of the pipet aperture and on the sample

velocity. Faster lateral movement and smaller aperture gives smaller width and depth of channels. One such channel is presented in Figure 2c, with width of  $\sim 340$  nm and depth of  $\sim 660$  nm, written with a 50 nm aperture pipet at a velocity of  $\sim 3 \mu\text{m/s}$ .

There are two surprising features in these experiments. One is the existence of “shoulders”, protrusions above the background surface, around the wells and on both sides of the channels (Figure 2b and 2d). The other is the fact that the line describing the dependence of the etched volume with time has a positive intercept at zero time (Figure 4b). In other words, there is a protrusion ( $\sim 0.16 \mu\text{m}^3$ ) at  $t = 0$ . In fact, both effects have a common reason, namely swelling of the protein substrate, as shown below.

We performed control experiments with water-filled pipets. These resulted in mounds when the sample was held in the same position (as opposed to wells when trypsin was present in the solution), or ridges when the sample was moved (as opposed to channels in the trypsin case). A mound created this way is shown in Figure 3a, where water was allowed to flow for a period of 120 s. A ridge created with water only is shown in Figure 3c. These protrusions are a result of swelling of the BSA film. In fact, this swelling is what allows trypsin to access the cleavage sites of the individual BSA molecules. Flowing water for increasing time durations results in taller and wider mounds, with volumes increasing roughly linearly with time (Figure 4a).

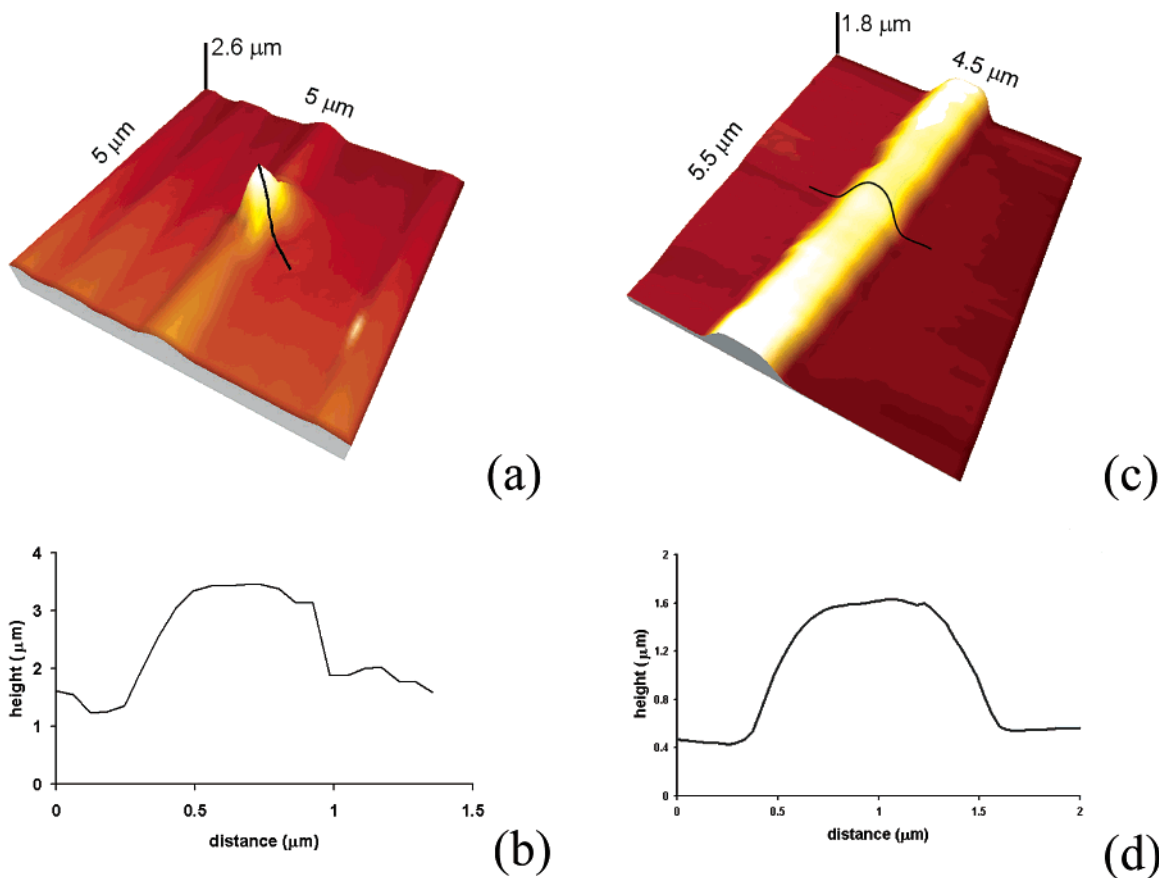


**Figure 3.** AFM images of features created by flowing pure water to the BSA substrate. (a) Mound created by flowing water through a 200 nm pipet for two minutes. (b) Cross-section of the mound in (a) along the line indicated, shows a width of  $0.75 \mu\text{m}$  and a height of  $2.3 \mu\text{m}$ . (c) Ridge created by flowing water through 200 nm pipet. (d) Cross-section of the ridge in (c) along the line indicated, shows a width of  $1.27 \mu\text{m}$  and a height of  $1 \mu\text{m}$ .

With these facts in mind, we suggest a comprehensive mechanism for the creation of the structures. Upon contact of the pipet with the sample, the trypsin solution wets the BSA substrate. The water causes an initial swelling of the BSA layer, thereby exposing lysine and arginine residues to the active trypsin sites, and allows further penetration of the trypsin solution into the BSA film. Upon cleavage into short oligopeptides, the three-dimensional structure of BSA collapses and a void is created. The process of etching is stopped by evaporation of the solution and drying of the trypsin, which then becomes inactive. The creation of depressions is the result of two competing effects: swelling (increasing positive volume) and etching (increasing negative volume) by the enzyme. Obviously, in the case presented, the rate of etching is higher than the rate of swelling, resulting in a net etching. The volumes of the wells, described in Figure 4b, are the result of this combined effect. Therefore, from the data about the swelling rate and the combined effect (Figure 4a,b, respectively), we can deduce the etching rate of trypsin. We plot the difference between the combined effect (Figure 4b) and the swelling (Figure 4a) in Figure 4c. From the slopes and intercepts of the linear regression lines fitted to the data points, it is visible that the swelling starts at  $t = 0$ , at a rate of  $\sim 0.0066 \mu\text{m}^3/\text{s}$ , trypsin activity starts some 6.8 s later at a rate of  $\sim 0.026 \mu\text{m}^3/\text{s}$ . The resulting, combined effect is a growing depression, which extends below the original

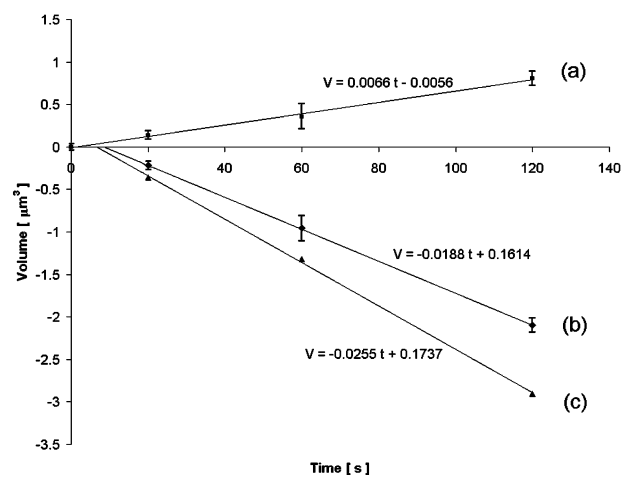


**Figure 4.** (a) Volumes of mounds, calculated from data as shown in Figure 3a,b, are linear with time of water flow. Linear regression yields a swelling rate of  $\sim 0.007 \mu\text{m}^3/\text{s}$ . Intercept is zero, within experimental error. Error bars indicate variation of four different mounds for each time point. (b) Volumes of wells, calculated from data as shown in Figure 2a,b are linear with the time of trypsin flow. Linear regression yields an etching rate of  $\sim 0.019 \mu\text{m}^3/\text{s}$ . Intercept predicts a protrusion of  $\sim 0.16 \mu\text{m}^3$  at  $t = 0$ . Time point for which  $V = 0$  is  $\sim 8.6$  s. Error bars indicate the variation of three different wells for each time point. (c) Deduced trypsin etching is calculated as the difference between the combined effect (b) and swelling (a). Linear regression yields an etching rate of  $\sim 0.026 \mu\text{m}^3/\text{s}$ . Time point for which  $V = 0$  is  $\sim 6.8$  s.



**Figure 5.** A series of images reproduced from a Monte Carlo simulation. The white portion represents the BSA substrate, dark gray represents the water drop, light gray dots within the drop represent trypsin molecules, and the black background represents air. The time-lapse snapshots show the various stages of trypsin etching of a BSA sample that has initially swollen. The times indicated are the iteration step of the simulation. Note the “shoulders” (indicated by arrows) that remain unetched on both sides of the resulting groove.

(unswollen) surface of the sample some 8.6 s from the initial pipet contact (some 2 s after trypsin starts cleaving the BSA), at a rate of  $\sim 0.019 \mu\text{m}^3/\text{s}$ . This is obviously a simplified model, however, it retains most of the important parameters of the process.

A Monte Carlo simulation starts with a drop of trypsin solution on top of a rectangular mound of BSA (representing the initial swelling of BSA). The algorithm simulates free diffusion of trypsin within the water drop, evaporation of water molecules from the surface of the drop, and collapse of BSA that is being met by a trypsin molecule. Not only does the simulation predict a roughly linear dependence of the etched volume with time, but it also provides the explanation for the “shoulders” observed in the AFM images. Due to the fact that the water molecules evaporate from the surface of the drop, its diameter decreases. Trypsin is forced toward the center of the hemisphere, thus increasing its concentration. This causes a preferential etching in areas below the center of the drop; thus, areas initially below the edges of the drop remain relatively untouched. These are the “shoulders” that we observe. A sequence of images reproduced from the computer simulation is presented in Figure 5 (movies of the simulation are available as Supporting Information).

An interesting conclusion resulting from this simplistic model is that the net effect of trypsin activity and swelling needs not always be a depression. If the trypsin etching rate is slower than the swelling rate, then no depressions are expected. Indeed, when reducing the trypsin concentration to half, the resulting features are mounds and ridges (image available as Supporting Information).

As a final demonstration of the combined effect described here, we performed writing with a solution of soybean trypsin inhibitor/trypsin in a ratio of 10:1. Again, the resulting features are positive volume mounds and ridges (image available as Supporting Information). Trypsin activity is inhibited, therefore the only effect is swelling. One can, in principle, use the inhibitor concentration as a tool to modulate trypsin activity. The existence of a specific inhibitor is obviously an additional benefit from using enzymes as etchants. This is a double specific recognition system, where the enzyme recognizes its substrate and the inhibitor recognizes its enzyme.

We have shown for the first time the use of a proteolytic enzyme to etch nanometer-scale depressions in a protein surface. We suggested a mechanism explaining the experi-

mental data, which contributes to the understanding of the processes. This enabled us to define the parameters governing these processes and control them. We believe that this approach has a great potential to create complex, three-dimensional features by wisely choosing enzymes and substrates with predesigned cleavage sites. By taking advantage of the wide spectrum of specific enzyme–substrate interactions, one can envision possible applications such as nanofluidics with readily functional channels and wells, creation of masks for further processing of the underlying substrate (whether biological or other), and others, with unprecedented nanometric resolution.

**Acknowledgment.** This work has been partially supported by grant #346/00 from the Israel Science Foundation and grant #01-01-01328 from the Israel Ministry of Science, Culture and Sports.

**Supporting Information Available:** Amino acid sequence of bovine serum albumin (BSA). Movie showing real-time NFP writing. Ridge created using low concentration trypsin solution. Ridge created by using a solution of soybean trypsin inhibitor and trypsin. Movies of Monte Carlo simulation. This material is available free of charge via the Internet at <http://pubs.acs.org>.

## References

- (1) Seeman, N. C. *J. Theor. Biol.* **1982**, *99*, 237.
- (2) Braun, E.; Eichen, Y.; Sivan, U.; Ben-Yoseph, G. *Nature* **1998**, *391*, 775.
- (3) Lewis, A.; Kheifetz, Y.; Shambrodt, E.; Radko, A.; Khatchatryan, E.; Sukenik, C. *Appl. Phys. Lett.* **1999**, *75*, 2689.
- (4) Hong, M. H.; Kim, K. H.; Bae, J.; Jhe, W. *Appl. Phys. Lett.* **2000**, *77*, 2604.
- (5) Bruckbauer, A.; Ying, L. M.; Rothery, A. M.; Zhou, D. J.; Shevchuk, A. I.; Abell, C.; Korchev, Y. E.; Klenerman, D. *J. Am. Chem. Soc.* **2002**, *124*, 8810.
- (6) Taha, H.; Marks, R. S.; Gheber, L. A.; Rouso, I.; Newman, J.; Sukenik, C.; Lewis, A. *Appl. Phys. Lett.* **2003**, *83*, 1041.
- (7) Piner, R. D.; Zhu, J.; Xu, F.; Hong, S. H.; Mirkin, C. A. *Science* **1999**, *283*, 661.
- (8) Lee, K. B.; Park, S. J.; Mirkin, C. A.; Smith, J. C.; Mrksich, M. *Science* **2002**, *295*, 1702.
- (9) Liu, G. Y.; Amro, N. A. *Proc. Natl. Acad. Sci. U.S.A.* **2002**, *99*, 5165.
- (10) Li, Y.; Maynor, B. W.; Liu, J. *J. Am. Chem. Soc.* **2001**, *123*, 2105.
- (11) Demers, L. M.; Ginger, D. S.; Park, S. J.; Li, Z.; Chung, S. W.; Mirkin, C. A. *Science* **2002**, *296*, 1836.
- (12) Sun, S. Q.; Chong, K. S. L.; Leggett, G. J. *J. Am. Chem. Soc.* **2002**, *124*, 2414.
- (13) Philipona, C.; Chevlot, Y.; Leonard, D.; Mathieu, H. J.; Sigrist, H.; Marquis-Weible, F. *Bioconjugate Chem.* **2001**, *12*, 332.

NL034640M